

EXPERIMENTAL MODELING OF TSUNAMI BORE IMPINGEMENT ON A SIMPLIFIED COASTAL BUILDING

Wei-Liang Chuang, Texas A&M University, wliuchuang1986@tamu.edu

Kuang-An Chang, Texas A&M University, kchang@tamu.edu

James Kaihatu, Texas A&M University, jkaihatu@tamu.edu

Rodrigo Cienfuegos, Pontificia Universidad Catolica de Chile, racienfu@ing.puc.cl

Cyril Mokrani, Pontificia Universidad Catolica de Chile, cyrilmokrani@gmail.com

INTRODUCTION

Numerous laboratory efforts were devoted to improve our understanding to the process of tsunami wave-structure interaction and provide valuable data to validate numerical and analytical models. However, the highly turbulent and multiphase nature of tsunami bores makes the study of their impacts very challenging. Many experimental studies (e.g., Shafiei et al. 2016) employed wave gauges to measure the bore height and estimate the bore front velocity based on shallow water equations. Considering the complexity of the flow and its impact with structures, the conversion between the bore height and the bore velocity is far from straightforward. Therefore, this study attempts to apply the bubble image velocimetry (BIV, Ryu et al. 2005) technique to directly measure the flow velocities during the tsunami bore impact. A tsunami wave, that breaks on a sloping beach, propagates inland as a form of bore, and impinges on a rigid structure, is considered as the scenario of interest. The objective is to perform a comprehensive investigation on the bore-structure interaction by examining the fluid velocity, impact pressure, and surge force during the impact event with various structure headings.

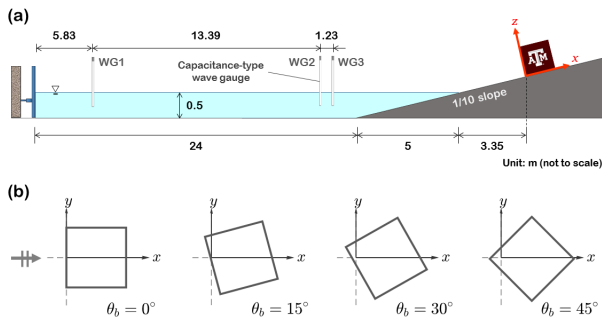


Figure1: Figure1: (a) Schematic diagram of the model setup and wave gauges. (b) four orientations and corresponding x-y coordinates.

EXPERIMENT SETUP

The experiment was performed in a three-dimensional wave basin housed in O.H. Hinsdale Wave Research Laboratory (HWRL) at Oregon State University. The wave basin was filled with fresh water to a constant depth of 0.50 m throughout the experiment. A simplified, rectangular coastal building was built and fixed on a 1/10 sloping beach. Four different heading orientations ($\theta_b = 0^\circ, 15^\circ, 30^\circ$ and 45°) of the model building were tested under the same wave condition. Figure 1 shows the model setup in the wave basin as well as the deployment of wave gauges and a sketch showing four different structure headings in basin-fixed coordinate system. A tsunami-like wave (similar to a solitary wave but with a

finite wave period) with an amplitude of 0.37 m was generated and designed to break on the sloping beach before reaching the model structure. A down-looking high speed camera was used to acquire images for the BIV velocity determination on the horizontal measurement plane. The BIV technique correlates the contrast texture created by air-water interface as tracers to determine the fluid velocities in an aerated region. Details of BIV technique can be found in Ryu et al. (2005). In addition to fluid velocity measurement, impact pressure on the frontal wall and surge force (parallel to the bore propagation) were measured by pressure sensors and a load cell, respectively. Note that the vertical array of pressure measurement points was set at the centerline of the model structure at zero-degree heading. The pictures of instrumentation are displayed in Fig. 2.

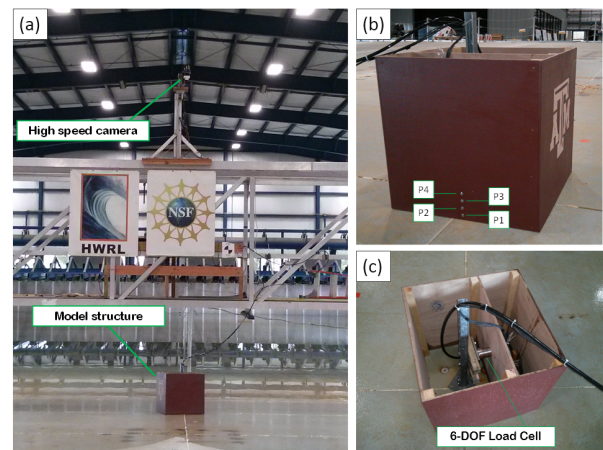


Figure 2: Pictures of the instrumentation of high speed camera (a), pressure sensors (b), and six-degree of freedom load cell (c).

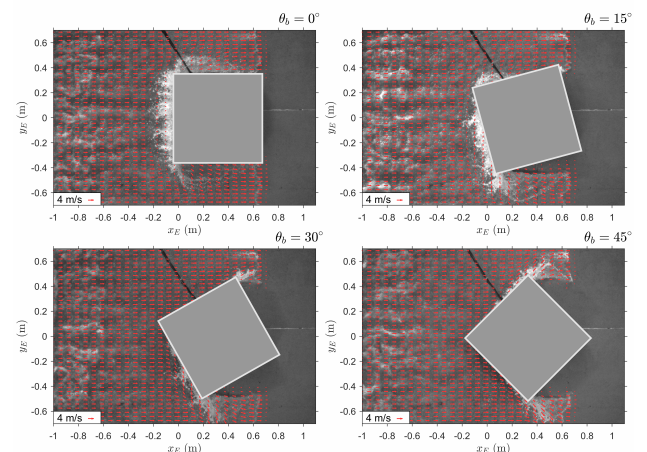


Figure 3: Mean fluid velocity maps around the structure at four different headings upon the bore impact.

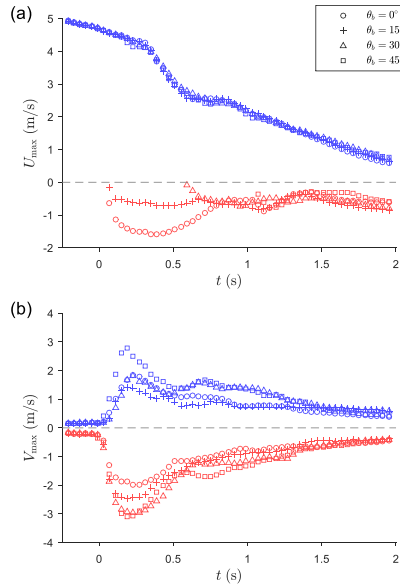


Figure 4: Temporal distributions of maximum positive (colored blue) and negative (colored red) U velocities (a) and V velocities (b) for the four headings

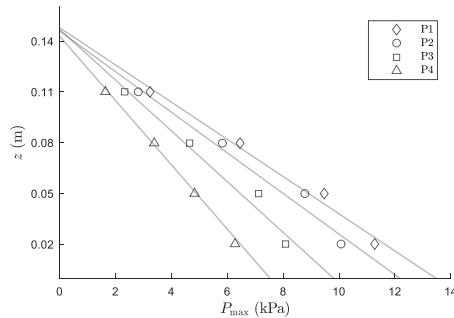


Figure 5: Vertical profiles of peak pressure for the four headings.

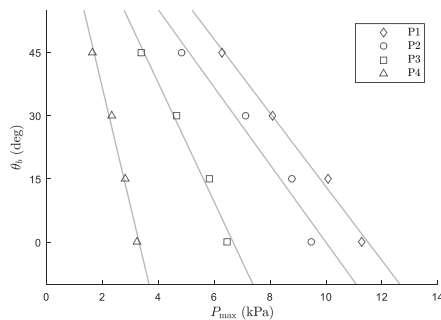


Figure 6: Peak pressure versus structure headings for the four elevations.

PRELIMINARY RESULTS

For each heading, the ensemble-averaged fluid velocity, impact pressure, and surge force was evaluated from 20 repeated tests with identical input wave condition. Figure 3 shows the mean velocity maps during the impact. Figure 4 presents the time history of maximum positive and negative U and V velocities; while the maximum V velocity were found at the 45° heading. Figure 5 plots the peak pressure against structure heading. In Fig. 4, it is observed that the peak pressure decreases as the structure more orientated. The vertical distribution of impact pressures is inversely proportional to the

elevation, with higher peak pressure near the bottom of the structure. In Fig. 6, a linear relationship is also found in the correlation between peak pressures and structure headings.

In this study, an attempt was given to model surge force as the sum of pressure integration and maximum static friction force. To account for the additional loading due to reverse flow, the reverse flow height was estimated by a formula derived by Robertson et al. (2013). The pressure measured at the top point was used to calculate the reverse flow loading by assuming constant pressure profile. The comparison between measured and calculated surge force is shown in Fig. 7. Although a good agreement in phase was found, the discrepancy in magnitude may indicate that current 1-D modeling is insufficient.

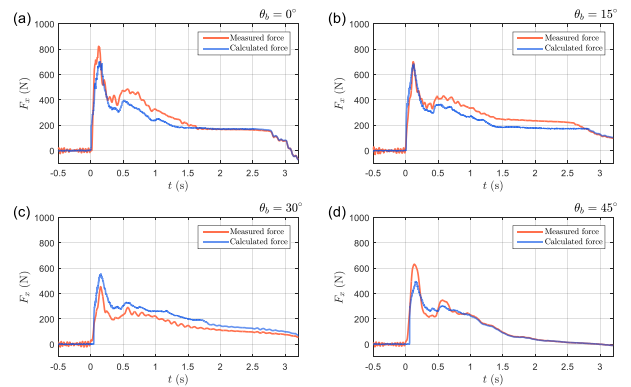


Figure 7: Comparison of calculated and measured surge force time histories for four different headings.

Comparison of the peak surge force ($F_{x,max}$) between measured and calculated results are further presented in Fig. 8. Calculated results include two approaches: first approach is finding the peak force in Fig. 5; and second approach is to calculate the force by using the linear profile of peak pressure observed in Fig. 5. The comparison indicates that the second approach, by excluding the average-out effect due to out-of-phase peak pressures, not only gives better approximation but also captures the large reduction of peak surge force at $\theta_b = 30^\circ$.

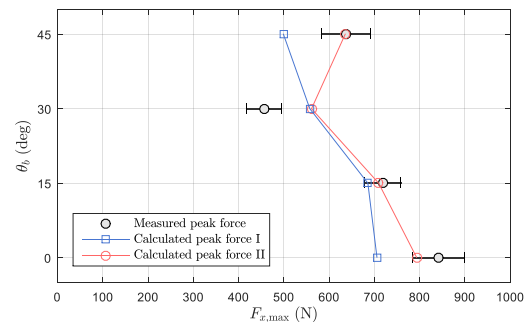


Figure 8: Comparison of measured and calculated surge forces.

REFERENCES

- [1] Robertson, I.N., Paczkowski, K., Riggs, H.R., and Mohamed, A. (2013) *Journal of Offshore Mechanics and Arctic Engineering*, 135(2), 021601.
- [2] Ryu, Y., Chang, K.-A., and Lim, H.-J. (2005) *Measurement Science and Technology*. 16:1945-

1953.

- [3] Shafiei, S., Melville, B. W., and Shamseldin, A. Y. (2016) *Coastal Engineering*, 110:1-16.